

## Ground state in the finite Dicke model for interacting qubits

R. A. Robles Robles,<sup>1</sup> S. A. Chilingaryan,<sup>2</sup> B. M. Rodríguez-Lara,<sup>1,\*</sup> and Ray-Kuang Lee<sup>3,4</sup>

<sup>1</sup>*Instituto Nacional de Astrofísica, Óptica y Electrónica, Calle Luis Enrique Erro No. 1, Sta. Ma. Tonantzintla, Pue. CP 72840, México*

<sup>2</sup>*Departamento de Física, Universidade Federal de Minas Gerais, Caixa Postal 702, 30123-970, Belo Horizonte, MG, Brazil*

<sup>3</sup>*Department of Physics, National Tsing-Hua University, Hsinchu 300, Taiwan, Republic of China*

<sup>4</sup>*Institute of Photonics Technologies, National Tsing-Hua University, Hsinchu 300, Taiwan, Republic of China*

(Received 15 September 2014; published 16 March 2015)

We study the ground state of a finite-size ensemble of interacting qubits driven by a quantum field. We find a maximally entangled  $W$  state in the ensemble part of the system for a certain region of the coupling parameters. The area of this region decreases as the ensemble size increases and, in the classical limit, becomes the line in parameter space that defines the phase transition of the system. In the classical limit, we also study the dynamics of the system and its transition from order to disorder for initial energies close to the ground-state energy. We find that a critical energy providing this transition is related to the minimum of the projection of the total angular momentum of the quantum system in the  $z$  direction.

DOI: [10.1103/PhysRevA.91.033819](https://doi.org/10.1103/PhysRevA.91.033819)

PACS number(s): 03.67.Bg, 03.75.Kk, 42.50.Pq

### I. INTRODUCTION

A set of  $N_q$  interacting qubits coupled to a quantized field may be described by the Hamiltonian

$$\hat{H} = \omega_f \hat{N} + \delta \hat{J}_z + \frac{\eta}{N_q} \hat{J}_z^2 + \frac{\lambda}{\sqrt{N_q}} (\hat{a} + \hat{a}^\dagger) \hat{J}_x, \quad (1)$$

where the detuning,  $\delta = \omega - \omega_f$ , is defined as the difference between the qubit transition frequency,  $\omega$ , and the quantized field frequency,  $\omega_f$ ; the field-ensemble and the interqubit coupling are given by the constants  $\lambda$  and  $\eta$ , respectively; the orbital angular momentum representation,  $J_i$  with  $i = x, y, z, \pm$ , such that  $[\hat{J}_i, \hat{J}_j] = i\epsilon_{ijk} \hat{J}_k$ , describes the qubit ensemble; the creation (annihilation) operators describe the field,  $\hat{a}^\dagger$  ( $\hat{a}$ ); and the total number of excitation in the system is given by the operator  $\hat{N} = \hat{a}^\dagger \hat{a} + \hat{J}_z + N_q/2$ . This model may be realized with trapped hyperfine ground states of a Bose-Einstein condensate inside a microwave cavity [1–4] or with arrays of interacting superconducting qubits coupled to the quantum field mode in a coplanar waveguide resonator [5] where a no-go theorem may [6] or may not [7] exist, or with coupled nitrogen vacancy centers interacting with a planar microwave cavity [8].

Beyond the fact that this Hamiltonian describes an experimentally feasible system that goes from integrable at  $\lambda = 0$  [9] to quasi-integrable at  $\eta = 0$  [10], our interest is twofold. First, this Hamiltonian is equivalent to the Lipkin-Meshkov-Glick (LMG) model [11] in the limit  $\lambda = 0$ . The LMG model produces maximal entanglement at the first-order (second-order) quantum phase transition of the ground state if the coupling is antiferromagnetic (ferromagnetic) [12,13]. The ground-state phase transition of the Hamiltonian in Eq. (1) has been studied in the thermodynamic limit,  $N_q \rightarrow \infty$ , within and without the rotating wave approximation (RWA) [2] and in the quantum regime, using coherent states for both the field and ensemble, without the RWA [3]; these results show the existence of a finite-size first-order quantum phase transition and a second-order super-radiant phase transition. Finite-size

quantum phase transitions in the ground state of the finite Dicke model have been associated with entanglement between the ensemble and the quantum field [14,15] and with bipartite entanglement among qubits due to finite-size effects [16–18]. Thus, for a sufficiently low field-ensemble coupling and an adequate interqubit coupling, it may be possible to obtain a maximally entangled state of the ensemble in the ground state of the system described by Eq. (1). Entanglement is a fundamental quantum mechanical phenomenon [19–23] and a precious resource in quantum information processing [24,25]. For a qubit ensemble, a  $W$  state [26] maximizes pairwise entanglement of formation [27,28] and is a robust source of entanglement [29,30]; i.e., it retains maximal bipartite quantum correlations whenever any pair of qubits are traced out. We will show that such a state is produced in the ground state of the Hamiltonian in Eq. (1) for a given parameter regime. Second, it has been recently shown that the finite-size Dicke model,  $\eta = 0$ , shows two excited-state quantum phase transitions; one for any given coupling at an energy rate  $2E/(\omega N_q) = 1$  [31,32] and another at the superradiant phase at an energy rate  $2E/(\omega N_q) = -1$  [33]. These transitions have been shown as peaks in the Peres lattice [34] of the system and a transition from order to disorder in the equivalent classical system has been shown around these energy rates [35]. The latter, the so-called excited-state quantum phase transition, is related to the unstable fixed points of the classical Dicke Hamiltonian. Some of us have shown the existence of stable and unstable fixed points that produce symmetric and asymmetric dynamics in the classical equivalent of Hamiltonian Eq. (1) under the RWA [36].

In the following, within the RWA and for weak interqubit coupling, we will show analytically that the maximal entanglement produced by the quantum phase transition in the Lipkin-Meshkov-Glick model is retained in the Dicke model for interacting qubits. Furthermore, for a fixed field-ensemble coupling,  $\lambda$ , the interqubit coupling,  $\eta$ , defines a series of first-order phase transitions related to the number of qubits in the ensemble,  $N_q$ , while, for a fixed interqubit coupling, there exists one second-order phase transition related to the couplings ratio [3] and a series of first-order transitions similar to those in the Dicke model under the RWA [16,17].

\*bmlara@inaoep.mx

Also, in Sec. II we will show analytically in the weak coupling regime, and numerically in general, that the inclusion of counterrotating terms does not erase the possibility of obtaining a maximally entangled multiqubit state. Then, in Sec. III, we will find the fixed points of the classical analog of the Dicke model for interacting qubits without the RWA and calculate the critical coupling parameter related to them; this parameter should be identical to that of the quantum case with an ensemble of infinite size. Also, we will show that a transition from order to disorder in the classical dynamics appears at exactly the value of the scaled energy corresponding to the minimum of the  $\hat{J}_z$  operator in the quantum system; in our case this scaled energy is  $2E/(\omega N_q) \geq -1$  and depends linearly on the size of the qubit ensemble.

## II. ENTANGLEMENT IN THE GROUND STATE

Here, we want to show that it is possible to find a maximally entangled  $W$  state in the ground state of our Hamiltonian model for a certain parameter set. For this reason, we need to start with the exact ground state in the RWA.

### A. Rotating wave approximation

The Hamiltonian in Eq. (1) under the RWA,

$$\hat{H}_{\text{RWA}} = \omega_f \hat{N} + \delta \hat{J}_z + \frac{\eta}{N_q} \hat{J}_z^2 + \frac{\lambda}{2\sqrt{N_q}} (\hat{a} \hat{J}_+ + \hat{a}^\dagger \hat{J}_-), \quad (2)$$

conserves the total number of excitations, thus the corresponding Hilbert space can be partitioned into subspaces where the Hamiltonian becomes a square matrix  $H^{(n)} = H_O^{(n)} + H_I^{(n)}$  with

$$H_O^{(n)} = \omega_f \left( n - \frac{N_q}{2} \right) \mathbb{I}_{\tilde{n}}, \quad (3)$$

$$(H_I^{(n)})_{i,j} = \delta_{i,j} d_i + \frac{\lambda}{2\sqrt{N_q}} (\delta_{i,j-1} o_j + \delta_{i,j+1} o_{j+1}), \quad (4)$$

where the identity matrix of rank  $d$  is given by  $\mathbb{I}_d$ , the row and column labels are in the range  $i, j = \tilde{n}, \tilde{n} + 1, \dots, n$ , where  $\tilde{n} = \max(0, n - N_q)$ , for the photon number  $n = 0, 1, 2, \dots$ . The symbol  $\delta_{i,j}$  stands for Kronecker  $\delta$ , and the diagonal and off-diagonal terms are defined as

$$d_j = \left( n - j - \frac{N_q}{2} \right) \left[ \delta + \frac{\eta}{N_q} \left( n - j - \frac{N_q}{2} \right) \right], \quad (5)$$

$$o_j = \sqrt{j(N_q + j - n)(n - j + 1)}. \quad (6)$$

In each subspace the square matrix is a tridiagonal symmetric real matrix with positive off-diagonal terms, i.e., a Jacobi matrix, and its eigenvalues can be found analytically [37–40]. The ground state of the system is found as the lowest eigenvalue for the set  $\{H^{(n)}\}$  for all values of  $n$ . Furthermore, a first-order quantum phase transition is located at the intersection of two ground-state energies belonging to contiguous subspaces.

The first ground-state structure, which we will call vacuum phase from now on, corresponds to the vacuum field and the

qubit ensemble state with zero excitation,

$$|\psi_g^{(0)}\rangle = |0\rangle \left| \frac{N_q}{2}, -\frac{N_q}{2} \right\rangle. \quad (7)$$

A first quantum phase transition, in a series of first-order quantum phase transitions, is found at the critical coupling strength,

$$\lambda_c = 2\sqrt{\left[ \omega + \left( \frac{1}{N_q} - 1 \right) \eta \right] \omega_f}, \quad (8)$$

with  $0 \leq \eta \leq N_q \omega / (N_q - 1)$ .

After this critical curve in parameter space, the ground state becomes

$$|\psi_g^{(1)}\rangle = c_0^{(1)} |0\rangle \left| \frac{N_q}{2}, 1 - \frac{N_q}{2} \right\rangle + c_1^{(1)} |1\rangle \left| \frac{N_q}{2}, -\frac{N_q}{2} \right\rangle. \quad (9)$$

The amplitudes are given by the expressions  $c_0^{(1)} = h/(h^2 + 1)^{1/2}$  and  $c_1^{(1)} = 1/(h^2 + 1)^{1/2}$  related to the amplitude parameter,

$$h = \frac{(1 - 1/N_q)\eta + \delta - \{4\lambda^2 + [(1 - 1/N_q)\eta - \delta]^2\}^{1/2}}{2\lambda}. \quad (10)$$

In this first nonvacuum phase, the ground state is fully separable,  $|\psi_g^{(1)}\rangle = |1\rangle |N_q/2, -N_q/2\rangle$ , in the limit  $h \rightarrow 0$ ; e.g., choosing  $\delta = 2\lambda$  when  $\lambda$  dominates. A second type of ground state occurs in the limit  $h \rightarrow \pm 1$ , where there is maximal entanglement between the field and the qubit ensemble,  $|\psi_g^{(1)}\rangle = (\pm|0\rangle |N_q/2, 1 - N_q/2\rangle + |1\rangle |N_q/2, -N_q/2\rangle) / \sqrt{2}$ ; e.g., the case  $h \rightarrow -1$  occurs when the field-ensemble coupling,  $\lambda$ , is dominant. And a third type, where the ground state of the whole system is separable,  $|\psi_g^{(1)}\rangle = |0\rangle |N_q/2, 1 - N_q/2\rangle$ , occurs in the limit  $h \rightarrow \infty$ , in other words when  $\lambda$  is small compared to the numerator of Eq. (10). Here, the ensemble part is maximally entangled as the qubit ensemble state  $|N_q/2, 1 - N_q/2\rangle$  is a  $W$  state. Note that the transition from one case to the other is continuous in this first nonvacuum ground state and any extended Dicke model that conserves the total number of excitations has a first nonvacuum phase of this form; e.g., a Dicke model that includes a quantized field nonlinearity [18]. Also, the following phase of the ground state,

$$|\psi_g^{(2)}\rangle = \sum_{j=0}^2 c_0^{(j)} |j\rangle \left| \frac{N_q}{2}, 2 - j - \frac{N_q}{2} \right\rangle, \quad (11)$$

will make the area for the first nonvacuum ground state smaller as the number of qubits in the ensemble grows. This may be a problem in the BEC realization where the size of the ensemble is large but this is not a problem in a circuit-QED realization where the number of qubits is small.

### B. Full model under weak couplings

Now, we want to show that the maximally entangled  $W$  state shown at the first nonvacuum phase survives the inclusion of counterrotating terms. We will use the unitary transformation,

$$\hat{U} = e^{-i\xi(\hat{a} + \hat{a}^\dagger)\hat{J}_y}, \quad \xi = \lambda N_q^{-1/2} / (\omega + \omega_f), \quad (12)$$

in the weak coupling regime,  $\lambda \ll \omega$ , such that  $\xi \ll 1$ . We will also require a weak intraensemble interaction,  $\eta \ll \omega$ , then it is possible to approximate,

$$\hat{H}_{\text{CR}} = \hat{U}^{-1} \hat{H} \hat{U},$$

$$\approx \omega_f \hat{a}^\dagger \hat{a} + \omega \hat{J}_z + \frac{\eta}{N_q} \hat{J}_z^2 + \frac{\tilde{\lambda}}{\sqrt{N_q}} (\hat{a} \hat{J}_+ + \hat{a}^\dagger \hat{J}_-), \quad (13)$$

with an auxiliary coupling strength  $\tilde{\lambda} = 2\omega_f \lambda / (\omega + \omega_f)$ . In other words, we have made an effective rotating wave approximation, and we already know that such a system has a first-order quantum phase transition at the critical value,

$$\lambda_c^{(\text{CR})} = (\omega + \omega_f) \sqrt{\frac{1}{\omega_f} \left[ \omega + \left( \frac{1}{N_q} - 1 \right) \eta \right]}. \quad (14)$$

Note that on resonance the expression for the first critical coupling in the weak coupling regime, Eq. (14), is equal to the critical coupling in the rotating wave approximation, Eq. (8). The ground state at the first nonvacuum phase is described again by Eq. (9) if we make the substitution  $\lambda \rightarrow \tilde{\lambda}$ . Then, the maximally entangled  $W$  state survives the inclusion of counterrotating terms for the region of interest, i.e., the weak coupling regime.

### C. Semiclassical analysis

Here we present a semiclassical analysis of the ground state just for the sake of completeness. In the Holstein-Primakoff representation of  $\text{SU}(2)$  [41] for a large number of qubits in the ensemble,  $\hat{J}_z = \hat{b}^\dagger \hat{b} - N_q/2$ ,  $\hat{J}_+ \approx \sqrt{N_q} \hat{b}^\dagger (1 - \hat{b}^\dagger \hat{b} / (2N_q))$ , and  $\hat{J}_- \approx \sqrt{N_q} (1 - \hat{b}^\dagger \hat{b} / (2N_q)) \hat{b}$ , the Hamiltonian in Eq. (1), up to a constant, reduces to

$$\hat{H} \approx \omega_f \hat{a}^\dagger \hat{a} + (\omega - \eta) \hat{b}^\dagger \hat{b} + \frac{\eta}{N_q} (\hat{b}^\dagger \hat{b})^2$$

$$+ \frac{\lambda}{2} (\hat{a}^\dagger + \hat{a}) \left[ \hat{b}^\dagger \left( 1 - \frac{\hat{b}^\dagger \hat{b}}{N_q} \right) + \left( 1 - \frac{\hat{b}^\dagger \hat{b}}{N_q} \right) \hat{b} \right]. \quad (15)$$

Thus, we can consider a coherent state for both the field and the qubit ensemble,  $|\alpha\rangle_f |\beta\rangle_q$ , to calculate the mean energy, up to a constant,

$$\langle \hat{H} \rangle \approx \omega |\alpha|^2 + \left[ \omega - \eta \left( 1 - \frac{|\beta|^2 - 1}{N_q} \right) \right] |\beta|^2$$

$$+ \frac{\lambda}{2} \left( 1 - \frac{|\beta|^2}{2N_q} \right) (\alpha + \alpha^*) (\beta + \beta^*). \quad (16)$$

In order to find the inflection points for this semiclassical energy, we derive with respect to the real and imaginary parts of both  $\alpha$  and  $\beta$  and solve the system  $\partial \langle \hat{H} \rangle / \partial x = 0$  with  $x = \alpha_R, \alpha_I, \beta_R, \beta_I$ . The trivial solution is the ground state  $|0\rangle_f |0\rangle_q$  and we check for intersections with the remaining six solutions, two of them do not intersect the ground state and the remaining four do it at the semiclassical critical coupling parameter,

$$\lambda_c^{(\text{SC})} = \sqrt{\left[ \omega + \left( \frac{1}{N_q} - 1 \right) \eta \right] \omega_f}, \quad (17)$$

$$= \frac{\lambda_c}{2}, \quad (18)$$

at which a second-order superradiant phase transition occurs [2,3]. It is half the critical strength found for the case without counterrotating terms,  $\lambda_c$  in Eq. (8), as expected from what happens for the Dicke model in the classical limit result, where accounting for counterrotating terms halves the critical coupling found without the counterrotating terms [42].

### D. Numerical analysis

In order to find the numerical ground state of the Hamiltonian in Eq. (1) we will follow a coherent state approach [43]. For this reason we will move to the frame defined by

$$|\psi\rangle = \hat{R}_y \left( \frac{\pi}{2} \right) \hat{D} \left( \frac{\tilde{\lambda}}{\omega_f} \hat{J}_z \right) |\xi\rangle, \quad (19)$$

with the rotation around  $\hat{J}_y$  given as  $\hat{R}_y(\varphi) = e^{i\varphi \hat{J}_y}$  and the displacement operator in the form  $\hat{D}(\beta \hat{\Delta}) = e^{\beta \hat{\Delta} \hat{a}^\dagger - \beta^* \hat{a} \hat{\Delta}}$ , with  $[\hat{\Delta}, \hat{a}] = 0$ , and the size-scaled coupling defined as  $\tilde{\lambda} = \lambda / \sqrt{N_q}$ . In the new frame, the system is ruled by an effective Hamiltonian,

$$\hat{H}_D = \hat{D}^\dagger \left( \frac{\tilde{\lambda}}{\omega_f} \hat{J}_z \right) \hat{R}_y^\dagger \left( \frac{\pi}{2} \right) \hat{H} \hat{R}_y \left( \frac{\pi}{2} \right) \hat{D} \left( \frac{\tilde{\lambda}}{\omega_f} \hat{J}_z \right), \quad (20)$$

$$= \omega_f \hat{a}^\dagger \hat{a} - \frac{\tilde{\lambda}^2}{\omega_f} \hat{J}_z^2 + \frac{\omega}{2} \left[ \hat{J}_+ \hat{D}^\dagger \left( \frac{\tilde{\lambda}}{\omega_f} \right) + \hat{J}_- \hat{D} \left( \frac{\tilde{\lambda}}{\omega_f} \right) \right]$$

$$+ \frac{\eta}{4N_q} \left[ \hat{J}_+ \hat{D}^\dagger \left( \frac{\tilde{\lambda}}{\omega_f} \right) + \hat{J}_- \hat{D} \left( \frac{\tilde{\lambda}}{\omega_f} \right) \right]^2, \quad (21)$$

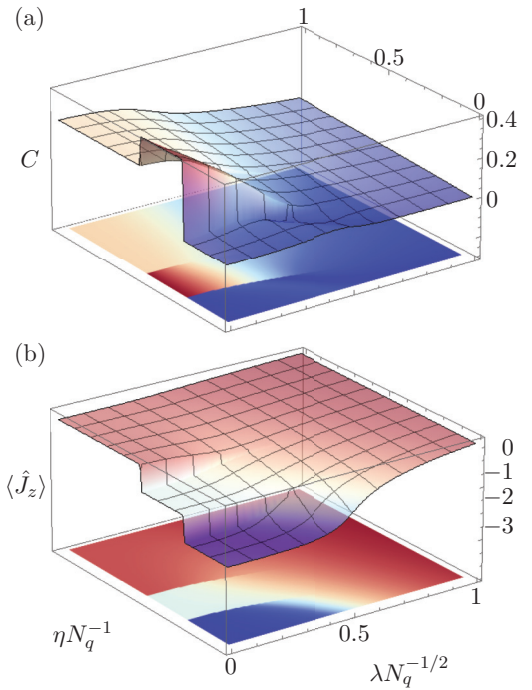


FIG. 1. (Color online) (a) Entangled web concurrence and (b) mean value of  $\hat{J}_z$  for the ground state of the model Hamiltonian in Eq. (1) with five qubits,  $N_q = 5$ , under off-resonant interaction with the quantized field,  $\omega_f = 0.75\omega$ . The qubit interaction,  $\eta$ , and field-ensemble coupling,  $\lambda$ , are given in units of the qubit transition frequency,  $\omega$ .

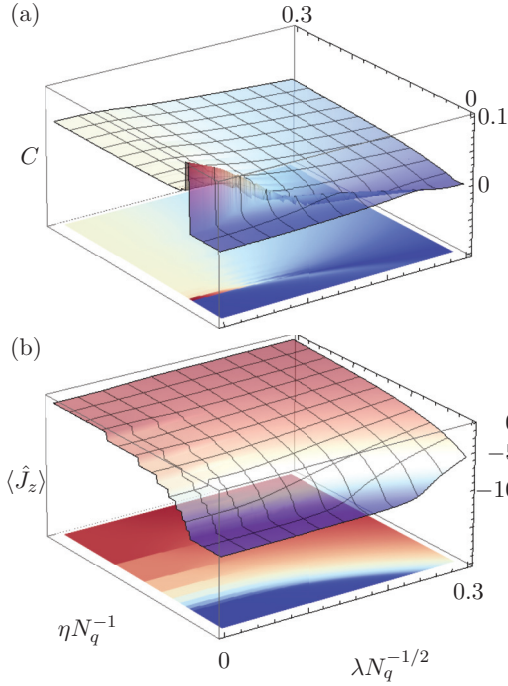


FIG. 2. (Color online) (a) Entangled web concurrence and (b) mean value of  $\hat{J}_z$  for the ground state of the model Hamiltonian in Eq. (1) with 20 qubits,  $N_q = 20$ , under resonant interaction with the quantized field,  $\omega_f = \omega$ . The qubit interaction,  $\eta$ , and field-ensemble coupling,  $\lambda$ , are given in units of the field frequency,  $\omega_f$ .

which is amenable to numerical diagonalization. In the following we show some numerical results that confirm our prediction of a maximally entangled qubit ensemble in the ground state of the model. Figures 1(a) and 2(a) show the concurrence,  $C$ , for the entangled web [27] of qubit ensembles with  $N_q = 5$  and  $N_q = 20$ , in that order. A maximum is reached in the first nonvacuum phase of the ground state and its value is the expected entangled web concurrence maximum of  $2/N_q$ . The critical coupling strength found in the RWA under weak coupling limit and in the semiclassical limit are in good agreement with the numerical results. Figures 1(b) and 2(b) show the mean value of  $\hat{J}_z$ . Note that a single excitation is present for the parameter region where maximum entanglement between the qubits is found as expected [27,28]. Figure 1 deals with an off-resonant case,  $\delta = 0.25$ , and Fig. 2 with the resonant case,  $\delta = 0$ .

### III. CLASSICAL ANALOG

We are also interested in the phase transition of our system related to the classical limit; i.e., making the substitution  $N_q \rightarrow \infty$  in the critical semiclassical coupling  $\lambda_c^{(SC)}$ . Some of us have found a relation between the critical value in the semiclassical limit and the transition for fixed points of the classical analog of interacting qubits driven by a quantum field under the RWA [36]. For this reason, we will explore the classical analog of our Hamiltonian, Eq. (1), which may be obtained by substituting the ensemble operators by the classical angular momentum canonical pair [44],  $\{j_z, \phi\}$ , and the field operators by the

classical harmonic oscillator canonical pair,  $\{p, q\}$ ,

$$\hat{a} \rightarrow \frac{1}{\sqrt{2}}(q + ip), \quad (22)$$

$$\hat{a}^\dagger \rightarrow \frac{1}{\sqrt{2}}(q - ip), \quad (23)$$

$$\hat{J}_z \rightarrow j_z, \quad (24)$$

$$\hat{J}_x \rightarrow \sqrt{j^2 - j_z^2} \cos \phi, \quad (25)$$

$$\hat{J}_y \rightarrow \sqrt{j^2 - j_z^2} \sin \phi, \quad (26)$$

where the variable  $\phi$  is the azimuthal angle of the Casimir vector  $\vec{j} = (j_x, j_y, j_z)$  of constant magnitude  $j = N_q/2$ . Thus, the equivalent classical Hamiltonian,

$$H = \frac{\omega_f}{2}(q^2 + p^2) + \omega j_z + \frac{\eta}{2j} j_z^2 + q\lambda\sqrt{j} \sqrt{1 - \frac{j_z^2}{j^2}} \cos \phi, \quad (27)$$

delivers the following equations of motion:

$$\frac{dq}{dt} = \omega_f p, \quad (28)$$

$$\frac{dp}{dt} = -\omega_f q - \lambda\sqrt{j} \sqrt{1 - \frac{j_z^2}{j^2}} \cos \phi, \quad (29)$$

$$\frac{d\phi}{dt} = \omega + \frac{j_z}{j} \left[ \eta - \frac{q\lambda \cos \phi}{\sqrt{j} \sqrt{1 - \frac{j_z^2}{j^2}}} \right], \quad (30)$$

$$\frac{dj_z}{dt} = q\lambda\sqrt{j} \sqrt{1 - \frac{j_z^2}{j^2}} \sin \phi. \quad (31)$$

#### A. Stable fixed points

We know from the quantum analysis that the vacuum field and the ensemble without excitation,

$$\{q, p, j_z, \phi\} = \{0, 0, -j, \phi\}, \quad (32)$$

is the ground state of the system with energy,

$$E(0, 0, -j, \phi) = -j \left( \omega - \frac{\eta}{2} \right). \quad (33)$$

Note that this set of variables is not a fixed point of the equations of motion. Now, our classical mechanics system has a different distribution of fixed points compared to noninteracting qubits [33]. In our case, a set of stable fixed points are given by the following parameters,

$$\{q, p, j_z, \phi\} = \{-q_{(s)}, 0, j_z^{(s)}, 0\}, \{q_{(s)}, 0, j_z^{(s)}, \pi\}, \quad (34)$$

with auxiliary definitions,

$$q_{(s)} = \frac{\lambda}{\omega_f} \sqrt{\frac{j^2 - (j_z^{(s)})^2}{j}}, \quad (35)$$

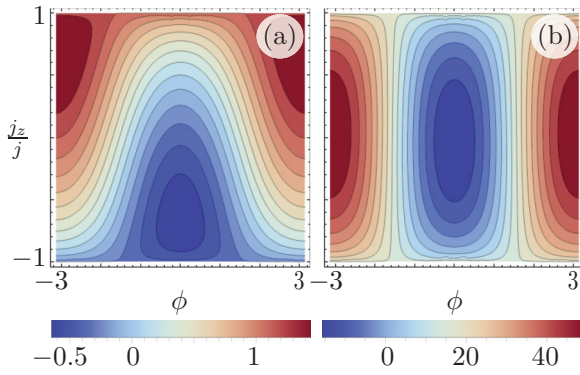


FIG. 3. (Color online) Energy landscape near the fixed points,  $q = q^{(s)}$  and  $p = 0$ , on resonance,  $\omega = \omega_f$ , and fixed interqubit coupling,  $\eta = 0.1\omega_f$ , for ensemble-field couplings (a)  $\lambda = 1.25\lambda_c^{(C)}$  and (b)  $\lambda = 6\lambda_c^{(C)}$ .

$$j_z^{(s)} = -\frac{j\omega\omega_f}{\lambda^2 + \eta\omega_f}, \quad (36)$$

and energy,

$$E(q^{(s)}, 0, j_z^{(s)}, 0) = -\frac{j}{2} \left[ \frac{\lambda^2}{\omega_f} + \frac{\omega^2\omega_f}{(\lambda^2 + \omega_f\eta)} \right]. \quad (37)$$

This energy and that for the set related to the quantum ground state before the phase transition intersect at the critical coupling,

$$\lambda_c^{(C)} = \sqrt{(\omega - \eta)\omega_f}, \quad (38)$$

$$= \frac{\lambda_c}{2} \Big|_{N_q \rightarrow \infty}, \quad (39)$$

i.e., it is just the semi-classical coupling found before for an ensemble of infinite size. Thus, we obtain the expected value for the critical coupling. Figure 3 shows the value of the Hamiltonian,

$$H(j_z, \phi) = \omega j_z + \frac{\eta}{2j} j_z^2 + \frac{\omega_f}{2} q_{(s)}^2 + \lambda q_{(s)} \sqrt{j} \sqrt{1 - \frac{j_z}{j}} \cos \phi, \quad (40)$$

for stable fixed points parameters,

$$\{q, p\} = \{q_{(s)}, 0\}, \quad (41)$$

for couplings above the critical coupling. It is straightforward to see that a global minimum is located in the south pole of the sphere,  $\{j, \theta, \phi\}$ , and moves toward the equator after crossing the critical value  $\lambda_c^{(C)}$ . Near the fixed points, it is possible to find stable periodical oscillations. These Rabi oscillations localize in a section of the available phase space for values close to the critical coupling; e.g., Fig. 3(a). Note that here the stable fixed points are simpler than those under the RWA [36] where one could immediately identify both a Rabi and Josephson regime.

So far, it has been shown that the classical Hamiltonian provides a landscape where stable Rabi oscillations may

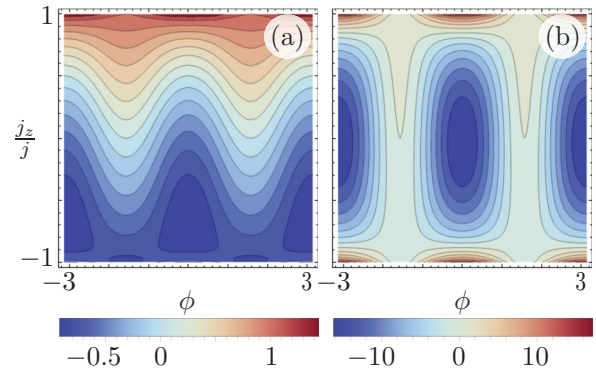


FIG. 4. (Color online) Energy landscape for parameter values,  $q = q^{(s)} \cos \phi$  and  $p = 0$ , on resonance,  $\omega = \omega_f$ , and fixed interqubit coupling,  $\eta = 0.1\omega_f$ , with ensemble-field couplings (a)  $\lambda = 1.25\lambda_c^{(C)}$  and (b)  $\lambda = 6\lambda_c^{(C)}$ .

appear. In order to explore the energy landscape far from the fixed point described above, we may choose the parameter values:

$$\{q, p\} = \{q_{(s)} \cos \phi, 0\}. \quad (42)$$

Such an approach allows us to see both global minima related to the two fixed points of the system, as shown in Fig. 4, but provides us with no further information. A rigorous analysis of the classical model may be of interest to study both stable and unstable fixed points, as it was done for the model under the RWA [36], but, at the moment, we will just focus on sampling initial conditions and their evolution in phase space near the energy minima.

## B. Order and disorder

It was recently shown that for noninteracting qubits there exists a transition from order to chaos for low-energy initial states [35]. Here we want to show that the addition of interaction between qubits conserves this behavior. But, more important, we want to point that, for a large ensemble, the transition from order to disorder near the ground state of the classical system is related to the energy at which the angular momentum projection  $j_z$  is minimum. Unfortunately, we are not able to provide an analytic value for this parameter, just numerical examples. Figure 5 shows Poincaré sections at  $p(t) = 0$  for a system with parameters  $j = 50$ ,  $\omega = \omega_f$ ,  $\eta = 0.1\omega_f$ , and  $\lambda = 1.25\lambda_c^{(SC)}$  and 40 random initial conditions with energy below [Fig. 5(a)], at [Fig. 5(b)], and above [Fig. 5(c)] the scaled energy  $E/(\omega j) = -0.951885$ . The scaled energy was calculated in the quantum model for a maximum number of 125 photons in the field. Note that below this critical scaled energy the system presents only stable orbits and the allowed phase state is restricted [Fig. 5(a)]. Then, at the critical scaled energy [Fig. 5(b)], there exists both stable and chaotic orbits and more of the phase space area is available. Finally, as the initial state energy becomes larger than the critical energy, more phase space is available and the stable orbits start to diminish in number [Fig. 5(c)]. This behavior was found in a sampling of different parameter sets above

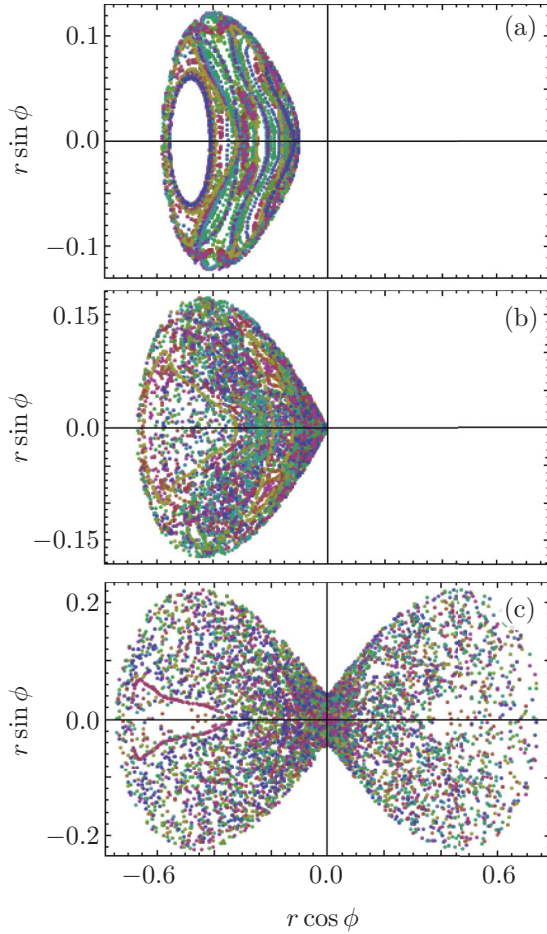


FIG. 5. (Color online) Poincaré sections for phase space  $\{r, \phi\}$  at  $p(t) = 0$  with  $r = 1 + j_z/j$  and initial scaled energies (a)  $E/(\omega j) = -0.99$ , (b)  $E/(\omega j) = -0.951\ 885$ , and (c)  $E/(\omega j) = -0.91$ . The parameter values used here are:  $j = 50$ ,  $\omega = \omega_f$ ,  $\eta = 0.1\omega_f$ ,  $\lambda = 1.25\lambda_c^{(SC)}$ . These deliver a minimum scaled angular momentum projection,  $\langle \hat{J}_z \rangle / (\omega j) = -0.828\ 784$ , with associated scaled energy  $E/(\omega j) = -0.951\ 885$  in the quantum case.

the semiclassical critical coupling,  $\lambda_c^{(SC)}$ . Now, this classical scaled energy corresponds to that of the quantum state with the minimum scaled value of  $\langle \hat{J}_z \rangle / (\omega j)$ .

Figure 6 shows the Peres lattice [34] given by the scaled angular momentum for the parameter set used in Fig. 5; note how the minimum does not correspond to the scaled energy value of  $-1$  found for the Dicke model [35]. Such behavior was confirmed numerically for different ensemble sizes and system parameters. For example, for the parameters mentioned above and varying the ensemble size, the quantum state that gives the minimum value of  $\langle \hat{J}_z \rangle$  has an energy that almost varies linearly in the ensemble size,  $N_q$ , as seen in Fig. 7. This was also confirmed for a sampling of different parameter sets slightly above the semiclassical critical coupling,  $\lambda_c^{(SC)}$ .

#### IV. CONCLUSIONS

We studied the ground state of a finite ensemble of interacting qubits driven by a quantum field. We found a specific parameter region that delivers a maximally entangled

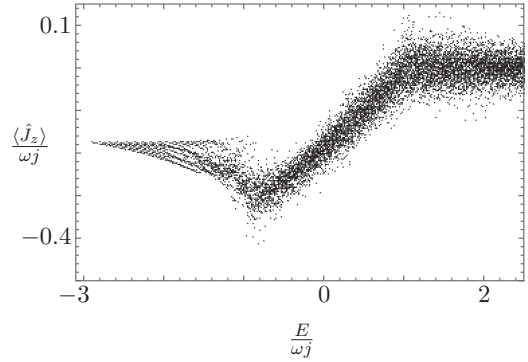


FIG. 6. Peres lattice of the scaled quantum angular momentum  $\langle \hat{J}_z \rangle / (\omega j)$  for the parameters  $\omega = \omega_f$ ,  $\eta = 0.1\omega_f$ ,  $\lambda = 1.25\lambda_c^{(SC)}$  and ensemble size  $N_q = 100$ .

$W$  state in the ground state of the ensemble. This parameter region corresponds to the first of a finite series of quantum phase transition in the ground state. As the ensemble size increases, the area of this first nonvacuum ground state decreases and, in the classical limit when the size of the ensemble is infinite, becomes the critical parameter defining the phase transition of the corresponding classical system.

In addition, while studying the classical analog of the model to find the phase transition, we find a critical energy at which there is a transition from order to disorder in the dynamics of the system. We numerically studied the behavior of different parameter sets and found that, in all cases studied, this critical energy is related to the energy of the quantum state that delivers the minimum value of  $\langle \hat{J}_z \rangle$  for each parameter set. This transition, which is related to an excited state, is interesting because it occurs for values close to the ground state and not

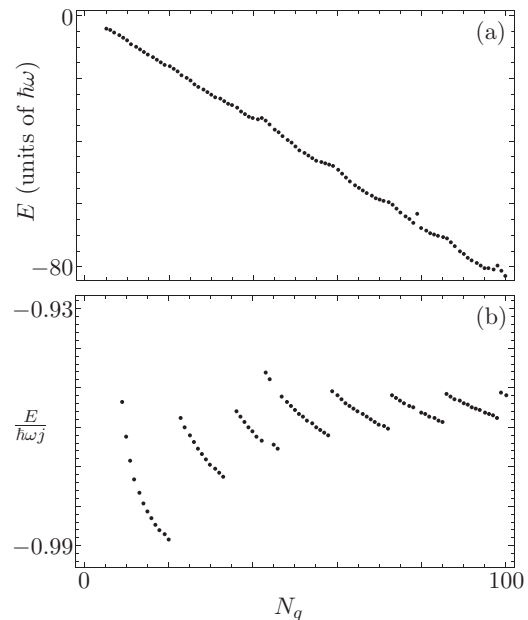


FIG. 7. (a) Energy and (b) scaled energy of the quantum state that delivers a minimum scaled angular momentum projection  $\langle \hat{J}_z \rangle / (\omega j)$  for the parameters  $\omega = \omega_f$ ,  $\eta = 0.1\omega_f$ ,  $\lambda = 1.25\lambda_c^{(SC)}$  and ensemble size  $N_q \in [5, 100]$ .

far from it as one would expect. We plan to extend our research regarding excited-state phase transitions of this model in the near future.

### ACKNOWLEDGMENTS

R.A.R.R. acknowledges financial support from CONACYT through the master degree scholarship No. 298009.

- 
- [1] G. Chen, J.-Q. Liang, and S. Jia, *Condens. Matter Phys.* **321**, 2 (2006).
- [2] G. Chen, Z. Chen, and J.-Q. Liang, *Europhys. Lett.* **80**, 40004 (2007).
- [3] Q.-H. Chen, T. Liu, Y.-Y. Zhang, and K.-L. Wang, *Phys. Rev. A* **82**, 053841 (2010).
- [4] D. Nagy, G. Szirmai, and P. Domokos, *Eur. Phys. J. D* **48**, 127 (2008).
- [5] G. Chen, Z. Chen, and J. Liang, *Phys. Rev. A* **76**, 055803 (2007).
- [6] O. Viehmann, J. von Delft, and F. Marquardt, *Phys. Rev. Lett.* **107**, 113602 (2011).
- [7] P. Nataf and C. Ciuti, *Nature Commun.* **1**, 72 (2010).
- [8] L. J. Zou, D. Marcos, S. Diehl, S. Putz, J. Schmiedmayer, J. Majer, and P. Rabl, *Phys. Rev. Lett.* **113**, 023603 (2014).
- [9] J. Dukelsky, G. G. Dussel, C. Esebbag, and S. Pittel, *Phys. Rev. Lett.* **93**, 050403 (2004).
- [10] C. Emary and T. Brandes, *Phys. Rev. Lett.* **90**, 044101 (2003).
- [11] H. J. Lipkin, N. Meshkov, and A. J. Glick, *Nucl. Phys.* **62**, 188 (1965).
- [12] J. Vidal, G. Palacios, and R. Mosseri, *Phys. Rev. A* **69**, 022107 (2004).
- [13] J. Vidal, R. Mosseri, and J. Dukelsky, *Phys. Rev. A* **69**, 054101 (2004).
- [14] N. Lambert, C. Emary, and T. Brandes, *Phys. Rev. Lett.* **92**, 073602 (2004).
- [15] J. Vidal and S. Dusuel, *Europhys. Lett.* **74**, 817 (2006).
- [16] V. Bužek, M. Orszag, and M. Roško, *Phys. Rev. Lett.* **94**, 163601 (2005).
- [17] O. Tsyplatyev and D. Loss, *J. Phys.: Conf. Ser.* **193**, 012134 (2009).
- [18] B. M. Rodríguez-Lara and R.-K. Lee, *J. Opt. Soc. Am. B* **27**, 2443 (2010).
- [19] E. Schrödinger, *Naturwissenschaften* **23**, 807 (1935).
- [20] E. Schrödinger, *Naturwissenschaften* **23**, 823 (1935).
- [21] E. Schrödinger, *Naturwissenschaften* **23**, 844 (1935).
- [22] A. Einstein, B. Podolsky, and N. Rosen, *Phys. Rev.* **47**, 777 (1935).
- [23] J. S. Bell, *Physics* **1**, 195 (1964).
- [24] M. A. Nielsen and I. L. Chuang, *Quantum Computation and Quantum Information* (Cambridge University Press, Cambridge, 2000).
- [25] J. Preskill, *J. Mod. Opt.* **47**, 127 (2000).
- [26] W. Dür, G. Vidal, and J. I. Cirac, *Phys. Rev. A* **62**, 062314 (2000).
- [27] M. Koashi, V. Bužek, and N. Imoto, *Phys. Rev. A* **62**, 050302 (2000).
- [28] W. Dür, *Phys. Rev. A* **63**, 020303 (2001).
- [29] H. J. Briegel and R. Raussendorf, *Phys. Rev. Lett.* **86**, 910 (2001).
- [30] A. Sen(De), U. Sen, M. Wieśniak, D. Kaszlikowski, and M. Zukowski, *Phys. Rev. A* **68**, 062306 (2003).
- [31] P. Pérez-Fernández, P. Cejnar, J. M. Arias, J. Dukelsky, J. E. García-Ramos, and A. Relaño, *Phys. Rev. A* **83**, 033802 (2011).
- [32] P. Pérez-Fernández, A. Relaño, J. M. Arias, P. Cejnar, J. Dukelsky, and J. E. García-Ramos, *Phys. Rev. E* **83**, 046208 (2011).
- [33] M. A. Bastarrachea-Magnani, S. Lerma-Hernández, and J. G. Hirsch, *Phys. Rev. A* **89**, 032101 (2014).
- [34] A. Peres, *Phys. Rev. Lett.* **53**, 1711 (1984).
- [35] M. A. Bastarrachea-Magnani, S. Lerma-Hernández, and J. G. Hirsch, *Phys. Rev. A* **89**, 032102 (2014).
- [36] B. M. Rodríguez-Lara and R.-K. Lee, *Phys. Rev. E* **84**, 016225 (2011).
- [37] J. D. Swalen and L. Pierce, *J. Math. Phys.* **2**, 736 (1961).
- [38] L. Pierce, *J. Math. Phys.* **2**, 740 (1961).
- [39] R. Haydock, V. Heine, and M. J. Kelly, *J. Phys. C: Solid State Phys.* **5**, 2845 (1972).
- [40] H. A. Yamani and M. S. Abdelmonem, *J. Phys. A: Math. Gen.* **30**, 2889 (1997).
- [41] J. Katriel, A. I. Solomon, G. D'Ariano, and M. Rasetti, *Phys. Rev. D* **34**, 2332 (1986).
- [42] H. J. Carmichael, C. W. Gardiner, and D. F. Walls, *Phys. Lett. A* **46**, 47 (1973).
- [43] Q.-H. Chen, Y.-Y. Zhang, T. Liu, and K.-L. Wang, *Phys. Rev. A* **78**, 051801(R) (2008).
- [44] M. A. M. de Aguiar, K. Furuya, C. H. Lewenkopf, and M. C. Nemes, *Ann. Phys.* **216**, 291 (1992).